JOURNAL OF MATERIALS SCIENCE: MATERIALS IN MEDICINE 13 (2002) 477–483

Mechanical effects of increases in the load applied in uniaxial and biaxial tensile testing. Part II. Porcine pericardium

J. M. GARCÍA PÁEZ, E. JORGE, A. ROCHA, J. L. CASTILLO-OLIVARES
Servicio de Cirugía Experimental, Clínica Puerta de Hierro, Madrid, Spain

I. MILLAN
Servicio de Bioestadística, Clínica Puerta de Hierro, Madrid, Spain

A. CARRERA, A. CORDON
Departamento de Mecánica Estructural y Resistencia de Materiales, Escuela Técnica Superior de Ingenieros Industriales, Madrid, Spain

G. TELLEZ, R. BURGOS
Servicio de Cirugía Cardiovascular, Clínica Puerta de Hierro, Madrid, Spain

The mechanical behavior of porcine pericardium was analyzed to compare it with that of calf pericardium employed in valve leaflets for cardiac bioprostheses. Forty samples of pericardium were subjected to uniaxial tensile testing, 20 as controls and 20 exposed to loads increasing stepwise from 0.5 to 1.5 kg and to 3 kg, and thereafter to rupture, with a return to zero load between each new increment. Another 20 samples were used in biaxial tensile tests involving the application of loads increasing stepwise (to 0.5, 1.5, 3 and 5 kg) until rupture with a zero-load interval before each increment. The ultimate stresses were very similar, showing no statistically significant differences when compared in terms of type of assay, controls and study samples or region of pericardial tissue being tested. In the stepwise biaxial assays, the mean stresses at rupture were also very homogeneous.

Using morphological and mechanical criteria for sample selection, it was possible to obtain mathematical fits for the stress/strain relationship, with excellent coefficients of determination.

The relationship between the area under the stress/strain curve and the load applied or the strain observed was also studied in the biaxial assay as an equivalent to the cycles of hysteresis produced in the test.

The increment in the area under the curve (the energy consumed) may be a good parameter for assessing the changes in the collagen fiber architecture of the pericardial tissue, changes that may help to detect early failure.

1. Introduction

Unlike calf pericardium, porcine pericardium has not been employed in the construction of bioprostheses or grafts [1–3]. The porcine bioprostheses used at the present time [4, 5] are native valves, properly sterilized and chemically stabilized to reduce their antigenicity [6–8]. As occurs with other cardiac bioprostheses, their durability is limited [4, 5, 9], although they offer every type of advantage over mechanical prostheses in terms of management and cost of maintenance because they do not require lifelong anticoagulation [10]. The lesser thickness of the porcine pericardium membrane suggests that valves made of this tissue would have lower mechanical resistance, this probably being the reason it is not utilized in the manufacture of these devices.

The resistance of a pericardial membrane has to do with its collagen fibers [11], their preferred direction [11, 12] and the degree of internal crosslinking following the chemical treatment employed to stabilize the tissue [6–8].

The elasticity depends on the elastic component formed by the elastic fibers and their distribution. However, pericardial tissue, whether bovine or porcine, exhibits a viscoelastic behavior [13, 14] that maintains the stress relaxation after the load applied is withdrawn [13, 15]. This stress relaxation, which exists with any load, is proportionally greater as the load decreases [16], and probably plays a very important role in the durability of any functional structure made of a biomaterial. It maintains a permanent deformation when the biomaterial is subjected to a low degree of stress, such as 0.20 MPa, similar to that reported for a cardiac valve leaflet under normal conditions in a living organism [17, 18].

Resistance and durability are two different concepts. For example, any suture is highly resistant to breakage [19], but sometimes this feature does not contribute much to the durability of a bioprosthesis. The deleterious effects of suture materials, in the form of shear stress that they exert on the valve leaflet, are well known [20, 21].

This study was designed to increase our knowledge of the mechanical behavior of porcine pericardium in the attempt to determine whether or not its resistance is actually lower than that of bovine pericardium. Using uniaxial and biaxial tests involving stepwise increments in load, we analyzed the stress/strain relationship when morphological and mechanical sample selection criteria [22] that ensure the homogeneity of the results were applied and when they were not. The return to zero load before each increment made it possible to observe the hysteresis exhibited by the biomaterial [13]. These cycles revealed the energy consumed at each level of load and, indirectly, the changes occurring within the pericardium and the shear stress produced [23].

The comparison of this behavior with that reported for calf pericardium will aid in a better understanding of these phenomena.

2. Material and methods

Porcine pericardium was obtained directly from a local abattoir. The pigs, which had been born and raised in Spain, were sacrificed between the ages of six and nine months. The tissue was transported to the laboratory in cold isotonic saline (0.9% sodium chloride) and cleaned. Then, each sac was mounted loosely on a 10-mm diameter ring, with the diaphragmatic attachment in the center and the sternopericardial ligaments on the circumference. For uniaxial tensile testing, four rectangular membranes measuring 8 cm long and 1.5 cm wide were cut from each of 20 pericardial sacs, along the apex-to-root axis as shown in Fig. 1. To perform the biaxial trials, two circular membranes measuring 2 cm in diameter were also cut from each pericardial sac, again as shown in Fig. 1. Both the rectangular and circular membrane pairs were comprised of one sample from the left side (region C) and one from the right side (region B) of the apex-to-root axis.

The thickness of each tissue fragment was determined by measuring a series of ten points, using a Mitutoyo micrometer (Elecount, series E:A33/8 Digital) with a precision at 20 °C of $\pm$ 3 µm. All of the trials were carried out at a room temperature of 22 to 24 °C.

All the membranes were treated for 24 h with 0.625% glutaraldehyde (pH 7.4) prepared from a commercially available solution of 25% glutaraldehyde (Merck) at a ratio of 1/50 (w/v), in 0.1 M sodium phosphate buffer.

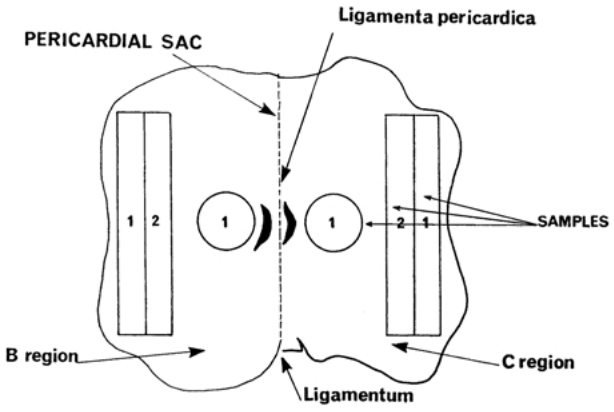

Figure 1 Open pericardial sac from which the samples were obtained. Circular sample (1) for stepwise biaxial trials: Rectangular samples (1 and 2) for control and stepwise uniaxial trials, respectively. Region B, pericardium corresponding to right ventricle, region C to left ventricle.

2.1. Uniaxial trials

For the control study, 10 rectangular tissue samples from the left side of the sac (region C) and 10 from the right (region B) were subjected to tensile testing in the direction of the longitudinal axis (root-to-apex) until rupture.

Another group of 20 rectangular tissue samples (10 from the left side of the sac and 10 from the right) was subjected to a similar uniaxial tensile test that differed only in that the increase in load was stepwise (starting at a mean load of 0.5 kg and increasing to mean loads of 1.5 and 3 kg, after which the load was incremented until rupture), with a return to zero load between each step.

These trials were performed on an Instron TTG4 tensile tester (Instron Ltd., High Wycombe, Buck, England) which records tensile stress under varying loads. The samples were clamped in such a way as to leave a free lumen of 45 mm. The results were recorded graphically, showing the load/strain (or load/deformation) diagram necessary to be able to calculate the stress/strain curve. The tensile stress of the pericardium was calculated taking into account the minor section.

2.2. Biaxial trials

The 20 circular membranes (10 from the left side of the sac and 10 from the right) underwent the same stepwise increments in mean load from 0.5 to 1.5, 3 and 5 kg, and thereafter to rupture, but were subjected to biaxial tensile stress produced by a hydraulic simulator (Fig. 2) capable of delivering increasing stresses to the porcine pericardial membranes secured with pressure clips. The membranes were exposed to increasing hydrostatic pressure caused by the compression transmitted to saline solution by a piston. As the piston moved, the fluid deformed the membrane and a pressure gauge determined the pressure, ranging between 0 and 16

Figure 2 Partial view of the hydraulic simulator.

atmospheres. The simulator consisted basically of a unit for measuring pressure equipped with a servomotor to drive the pump propelling the piston.

2.3. General description of the function of the system

A piston is activated by means of a digital monitor based on a high-speed processor that controls the direct current electric servomotor. The piston compresses the fluid and the pericardial membrane resists the pressure. The biomaterial is subjected to loads that are incremented stepwise four times, with a return to zero load prior to each new step, and thereafter, in a fifth step, increased continuously until rupture.

The controlling computer indicates the angular velocity of the activating system, which is maintained throughout the trial. The data acquisition system evaluates the fluid pressure and the movement of the piston at all times. The numerical data corresponding to these variables are transferred to a computer via a series interface, and stored for subsequent analysis.

2.4. Technical features of the hydraulic simulator

The most relevant technical specifications are as follows:

Amplifier. D-MOS technology; H-bridge configuration; maximum working voltage: 53 V; maximum intensity in steady state: 3 A.

Motor. Rated voltage: 24 DCV; rated output: 15 W; starting torque: 120 mN m; current in a vacuum: 21.7 mA; starting current: 3040 mA; maximum permanent torque: 30.46 mN m.

Incremental position sensor. Optical; two quadrature outputs and index impulse.

Quadrature processor. Programmable logic technology; two quadrature inputs; incremental/decremental monopolar impulse output; maximum working frequency of 4 MHz.

Digital compensator. Processor, RISC microcontroller, 24 MHz, 8 bits, 200 ns/instruction; maximum sampling frequency of 1 kHz; velocity range from 00 to 8 388 607 counts/sampling period $\times$ 256; proportional action coefficient (KP) of $-32\,768$–$32\,767$; differential action coefficient (KD) of $-32\,768$–$32\,767$.

Piston. 160-mm stroke; 32 mm in diameter; maximum pressure 16 atm.

Pressure sensor. Maximum pressure 16 atm; output signal: 4–20 mA.

Computer. Standard Pentium-75 configuration.

This system was developed by Sat Polar, S.L., a Spanish electronic engineering firm.

2.5. Tensile strength

Once the stress withstood by the pericardial membrane at each instant of the trial was known, its tensile strength was calculated using the Laplace equation for a thin-walled membrane subjected to pressure: $T_s = pr/2e$, where p is the pressure in kg/cm^2, r the radius of the membrane expressed in cm, e the thickness of the membrane in cm and T_s the tensile strength in kg/cm^2. To convert this value to MPa, we divided the result by 10.19.

2.6. Strain (deformation)

The movement of the piston indicated the variation in the fluid volume at every moment and for each different stress applied and, thus, the changes in membrane geometry up to the moment of rupture. At that point, the shape was that of a round dome, the base of which was a known circle (the frame on which the membrane to be tested was mounted). By measuring the changes in length of the longest arc of the dome, it was possible to determine the percentage of deformation, or strain, at each moment of the trial.

2.7. Statistical study and mathematical analysis comparison of means at rupture

The mean values at rupture for the three series of samples were compared, taking into account the different regions (B and C), by means of analysis of variance (ANOVA) and the Newman–Keuls test for multiple comparisons.

2.8. Mathematical fit of the tensile strength/deformation ratio

The tensile strength (MPa)/strain (per unit deformation) ratio was studied using the least squares method. The best fit corresponded to a third-order polynomial, the shape of which is expressed as $y = a_1x + a_2x^2 + a_3x^3$, where y is the tensile strength or stress in MPa and x is the per unit deformation (strain) of the membrane. The value of the constant a_0 was made to equal zero since due to biological considerations, the equation must pass through the origin (at zero tensile strength, there would be no deformation). For similar considerations, the analysis was done for $x \leq 0.20$ (the behavior of the function when the membrane could have surpassed its elastic limit, entering the realm of irreversible deformation, was not considered to be of interest).

2.9. Mean overall fit for each set of samples in each of the two regions

The stress/strain ratio was also studied by region within each series of samples.

2.9.1. Selection criteria

Selection criteria were established to ensure greater homogeneity of the samples. The purpose of these statistical selection criteria was to determine the probability that each membrane tested actually belonged to the region to which it was assigned in the initial selection. Thus, those membranes with a minimum thickness greater than the mean value for the corresponding series and region plus one standard deviation or less than the mean value minus one standard deviation were excluded, as were those membranes in which the difference between the mean thickness of a given region in each series and the minimum thickness for the corresponding region was greater than the mean value

TABLE I Mean stresses at rupture in control and stepwise uniaxial trials and stepwise biaxial trials

Type of trial	No. of samples	Region	Mean values at rupture (MPa)	Standard deviation	Range
Uniaxial					
Control	10	B	21.88	3.96	15.60–30.90
	10	C	23.29	6.39	7.40–29.50
				4.15	17.74–28.97
Stepwise	10	B	23.34	5.80	10.82–29.05
	10	C	19.66		
Biaxial					
Stepwise	10	B	61.15	23.31	15.80–98.80
	10	C	67.12	37.46	12.30–120.0

Stepwise trials consisted of a specific number of stepwise increases in load separated by decreases to zero load, after which the load was increased steadily until sample fracture. Region B: pericardium covering right ventricle. Region C: pericardium covering left ventricle.

for this difference as determined in the corresponding set, plus one standard deviation, indicating a lack of homogeneity.

In the uniaxial trials, the pairs of samples (one each from regions C and B) in which the stress (MPa) for $x = 0.20$ in the membrane cut from region B (right side of the pericardial sac) was above or below the mean plus or minus one standard deviation for said region were also excluded.

In the trials involving stepwise increases in load, those pairs of samples in which the tensile stress (MPa) reached in the first increment was higher or lower than the mean value for the corresponding series and region, plus or minus one standard deviation, were excluded.

2.9.2. Mean overall fit for the selected samples

On the basis of the aforementioned selection criteria, the following nine pairs were selected for each assay, representing 30.0% of all the samples assayed:

Control uniaxial trial: pairs nos. 3, 5 and 6.
Stepwise uniaxial trial: pairs nos. 6, 7 and 10.
Stepwise biaxial trial: pairs nos. 6, 8 and 9.

2.9.3. Hysteresis

The energy consumed in each cycle or step is referred to as hysteresis. The analysis of the results of the biaxial trial included the estimation of the function that related the area under the stress/strain curve to the stress applied or the strain produced, respectively.

3. Results

3.1. Rupture

The stresses at rupture are shown in Table I. In the uniaxial trials, the mean values obtained at rupture ranged between 19.66 and 23.88 MPa. There were no statistically significant differences with respect to type of assay (control or stepwise load increases) or region (B or C). In the biaxial trial, the mean values at rupture were 61.16 and 67.12 MPa for regions B and C, respectively. The differences between the mean ultimate stresses in the uniaxial and biaxial trials were statistically significant ($p < 0.001$).

TABLE II Values for the equation fitting the stress/strain curve ($y = a_1x + a_2x^2 + a_3x^3$) and R^2 in the control uniaxial trial without and with the application of sample selection criteria

Samples	a_1	a_2	a_3	R^2
Region B				
Not selected	− 16.15	588.65	− 616.30	0.865
Selected	− 46.95	989.86	− 1326.60	0.976
Region C				
Not selected	24.32	390.19	− 558.99	0.803
Selected	− 20.46	651.69	− 523.26	0.953

$y = a_1x + a_2x^2 + a_3x^3$, where y is the area under the stress/strain curve and x is the stress or the strain, respectively.
R^2: coefficient of determination. Region B: pericardium covering right ventricle. Region C: pericardium covering left ventricle.

3.2. Mathematical fit of the stress/strain curve

Table II shows the results of this fit in the control uniaxial trial both when sample selection criteria were not applied and when they were. After sample selection, the coefficients of determination (R^2) ranged between 0.865 and 0.976 in region B and 0.803 and 0.953 in region C. The mathematical fits of the stress/strain curves for each increment in load and the corresponding no-load interval until rupture, without and with the application of the selection criteria appear in Tables III and IV, respectively. In the trials in which the selection criteria were not employed, the coefficients of determination (R^2) ranged between 0.623 and 0.978, while those observed after application of the selection criteria ranged from 0.797 to 0.999.

TABLE III Values for the equation fitting the stress/strain curve ($y = a_1x + a_2x^2 + a_3x^3$) and R^2 in the stepwise uniaxial trial without application of sample selection criteria

Load changes	a_1	a_2	a_3	R^2
Region B				
1st increase	38.58	− 240.70	489.89	0.806
Zero load	56.74	− 568.29	1766.07	0.772
2nd increase	17.33	587.84	− 2917.30	0.786
Zero load	52.26	− 117.11	68.06	0.759
3rd increase	− 47.49	1764.85	− 5342.60	0.834
Zero load	26.06	367.47	− 450.02	0.788
4th increase/ rupture	− 129.08	3178.84	− 9697.60	0.915
Region C				
1st increase	− 5.60	540.36	− 2005.50	0.777
Zero load	8.00	211.03	− 685.24	0.623
2nd increase	51.34	− 31.97	− 32.71	0.762
Zero load	60.01	− 115.02	58.16	0.762
3rd increase	− 48.60	1491.30	− 1158.00	0.974
Zero load	− 89.05	1784.76	− 1738.50	0.965
4th increase/ rupture	− 72.36	2013.10	− 2816.50	0.978

$y = a_1x + a_2x^2 + a_3x^3$, where y is the area under the stress/strain curve and x is the stress or the strain, respectively.
For a brief description of stepwise trials, see Table I. Loads: 0.5, 1.5 and 3 kg, return to 3 kg/increase until rupture.
R^2: coefficient of determination. Region B: pericardium covering right ventricle. Region C: pericardium covering left ventricle.

TABLE IV Values for the equation fitting the stress/strain curve ($y = a_1x + a_2x^2 + a_3x^3$) and R^2 in the stepwise uniaxial trial with the application of sample selection criteria

Load changes	a_1	a_2	a_3	R^2
Region B				
1st increase	4.09	352.64	− 1865.80	0.871
Zero load	8.08	253.11	− 1435.80	0.838
2nd increase	36.12	466.55	− 3287.60	0.801
Zero load	− 0.18	1048.58	− 5599.10	0.797
3rd increase	− 41.80	1728.29	− 5125.80	0.866
Zero load	− 23.40	740.45	− 1612.40	0.851
4th increase/ rupture	− 105.97	3005.11	− 9096.80	0.928
Region C				
1st increase	− 26.302	1235.70	− 6603.50	0.954
Zero load	− 86.326	2456.58	− 13 030.00	0.932
2nd increase	− 9.517	881.68	− 305.89	0.971
Zero load	− 10.483	158.24	5000.29	0.936
3rd increase	− 48.637	1574.95	− 2022.60	0.970
Zero load	− 46.023	358.82	7048.92	0.999
4th increase/ rupture	− 63.084	1522.42	66.83	0.991

$y = a_1x + a_2x^2 + a_3x^3$, where y is the area under the stress/strain curve and x is the stress or the strain, respectively.

For a brief description of stepwise trials, see Table I. Loads: 0.5, 1.5 and 3 kg, return to 3 kg/increase until rupture.

R^2: coefficient of determination. Region B: pericardium covering right ventricle. Region C: pericardium covering left ventricle.

TABLE V Values for the equation fitting the stress/strain curve ($y = a_1x + a_2x^2 + a_3x^3$) and R^2 in the stepwise biaxial trial without the application of sample selection criteria

Load changes	a_1	a_2	a_3	R^2
Region B				
1st increase	3.63	− 2.03	1.14	0.921
Zero load	− 1.90	4.67	− 0.85	0.923
2nd increase	4.96	− 4.48	2.12	0.932
Zero load	5.31	− 5.29	2.37	0.936
3rd increase	9.32	− 10.04	3.73	0.939
Zero load	10.32	− 11.16	3.99	0.936
4th increase	16.48	− 17.94	5.79	0.926
Zero load	14.24	− 15.60	5.19	0.911
5th increase/ rupture	22.74	− 24.34	7.29	0.916
Region C				
1st increase	2.92	− 0.11	0.02	0.900
Zero load	4.06	− 1.01	0.18	0.902
2nd increase	1.40	1.71	− 0.24	0.807
Zero load	2.21	1.12	− 0.15	0.812
3rd increase	− 9.57	10.93	− 1.83	0.808
Zero load	− 4.94	7.19	− 1.24	0.747
4th increase	− 24.77	23.09	− 3.95	0.729
Zero load	9.09	− 11.09	4.36	0.895
5th increase/ rupture	28.61	− 31.30	9.29	0.888

$y = a_1x + a_2x^2 + a_3x^3$, where y is the area under the stress/strain curve and x is the stress or the strain, respectively.

For a brief description of stepwise trials, see Table I. Loads: 0.5, 1.5, 3 and 5 kg, return to 5 kg/increase until rupture.

R^2: coefficient of determination. Region B: pericardium covering right ventricle. Region C: pericardium covering left ventricle.

Tables V and VI show the fits of the stress/strain curves for the biaxial trials without and with selection criteria, respectively. When these criteria were not applied, the coefficients of determination (R^2) ranged from 0.729 to 0.939, findings that increased to between 0.930 and 0.999 when the selection criteria were employed.

TABLE VI Values for the equation fitting the stress/strain curve ($y = a_1x + a_2x^2 + a_3x^3$) and R^2 in the stepwise biaxial trial with the application of sample selection criteria

Load changes	a_1	a_2	a_3	R^2
Region B				
1st increase	5.06	− 4.53	2.23	0.993
Zero load	5.16	− 4.64	2.26	0.994
2nd increase	9.29	− 9.78	3.81	0.989
Zero load	8.18	− 8.61	3.44	0.984
3rd increase	13.33	− 14.57	5.08	0.980
Zero load	13.95	− 15.29	5.24	0.977
4th increase	24.96	− 27.15	8.30	0.967
Zero load	27.68	− 29.62	8.84	0.989
5th increase/rupture	50.15	− 51.39	13.79	0.991
Region C				
1st increase	2.15	0.66	− 0.082	0.937
Zero load	2.44	0.33	− 0.006	0.938
2nd increase	− 0.12	2.67	− 0.271	0.894
Zero load	0.03	2.44	− 0.222	0.893
3rd increase	16.41	− 18.09	6.075	0.984
Zero load	− 5.52	7.04	− 1.002	0.847
4th increase	27.95	− 30.46	9.218	0.973
Zero load	12.49	− 13.57	4.558	0.900
5th increase/rupture	31.89	− 32.70	8.839	0.836

$y = a_1x + a_2x^2 + a_3x^3$, where y is the area under the stress/strain curve and x is the stress or the strain, respectively.

For a brief description of stepwise trials, see Table I. Loads: 0.5, 1.5, 3 and 5 kg, return to 5 kg/increase until rupture.

R^2: coefficient of determination. Region B: pericardium covering right ventricle. Region C: pericardium covering left ventricle.

3.3. Hysteresis

The best estimation of the curve representing the relationship between the area under the stress/strain curve and the stress applied was a third-order polynomial with coefficients of determination (R^2) of 1.000 for region B and 0.999 for region C, although the coefficient a_3 can be considered negligible. The best estimation of the curve representing the relationship between the area under the stress/strain curve and the strain produced was a second-order polynomial with coefficients of determination (R^2) of 0.976 and 0.954 for regions B and C, respectively. These findings appear in Table VII and in Figs 3 and 4.

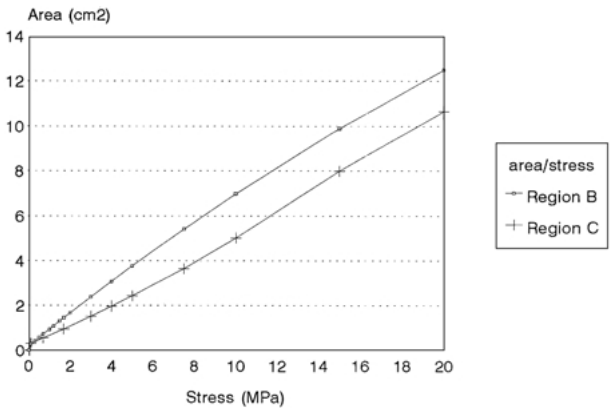

Figure 3 Curve representing the relationship between the area under the stress/strain curve and the stress applied.

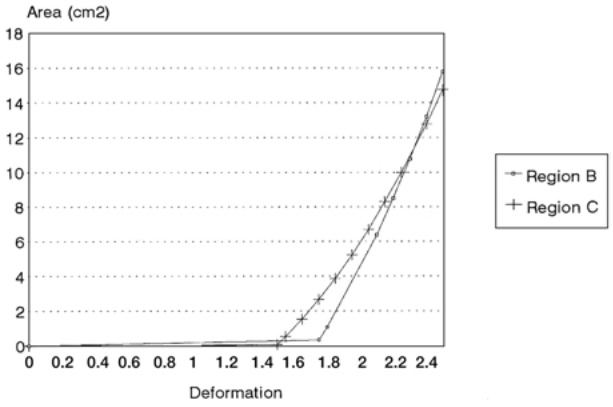

Figure 4 Curve representing the relationship between the area under the stress/strain curve and the strain produced.

TABLE VII Values for the equation fitting the curves representing the relationship between the area under the stress/strain curve and the stress and the strain, respectively and R^2 in the stepwise biaxial trial

Curve	a_1	a_2	a_3	R^2
Stress				
Region B	0.743	− 0.006	3×10^{-5}	1.000
Region C	0.394	0.008	− 0.0001	0.999
Strain				
Region B	− 14.116	8.17	—	0.976
Region C	− 8.745	5.86	—	0.954

$y = a_1x + a_2x^2 + a_3x^3$, where y is the area under the stress/strain curve and x is the stress or the strain, respectively.

R^2: coefficient of determination. Region B: pericardium covering right ventricle. Region C: pericardium covering left ventricle.

4. Discussion

As a parameter of the durability of a biomaterial, its resistance is merely orientational, although readily estimable. When a biomaterial with a given mechanical resistance is employed in the construction of a cardiac valve leaflet that is subjected to moderate or mild mechanical work, its durability should be much greater. This is the case of bioprostheses placed in tricuspid position [24, 25] and those implanted in aortic position in elderly patients [26, 27]. The resistance to rupture of porcine pericardium is in no way inferior to that of calf pericardium [22]. In uniaxial tensile testing, the mean stresses observed at rupture in porcine pericardium ranged between 19.66 and 23.34 MPa and, thus, were similar to those found in calf pericardium. In biaxial tests, the mean results at rupture were highly uniform in samples of pericardium from both the portion covering the right ventricle and that covering left ventricle (61.16 and 67.12 MPa for regions B and C, respectively). In contrast, in calf pericardium, there were marked differences between the mean values in the two regions (49.94 and 71.26 MPa, respectively). These findings may be explained by the smaller size of the porcine pericardial membrane and the failure to apply selection criteria to samples tested until rupture [22].

Thus, the hypothesis that porcine pericardium exhibits a lower resistance, at least to tensile testing until rupture, can be rejected.

The morphological and mechanical selection criteria applied [22] to enable the fit of the equations corresponding to the stress/strain relationship greatly enhanced the homogeneity of the results, ensuring the excellent fit of these equations. In the control uniaxial trial, the coefficients of determination (R^2) reached 0.865 to 0.976 in region B and 0.803 to 0.953 in region C.

In the stepwise uniaxial study, when the selection criteria were not applied, the mathematical fit of the results improved as each increment in the load took place. At the final level of load, the fit was excellent despite the omission of the method of selection, with coefficients of determination (R^2) of 0.915 and 0.978, respectively, for each region. This phenomenon, which was similar to that observed in calf pericardium, is related to the mechanical behavior and the direction of the collagen fibers when subjected to stress [11, 12]. When this stress is repeated, the collagen fibers, which are responsible for the mechanical resistance of the biomaterial [11], appear to align themselves with the axis of the stretch force.

This phenomenon is not encountered in the stepwise biaxial trial. The increasing loads do not improve the mathematical fits, but tissue selection does. The determination coefficients (R^2) ranged between 0.729 and 0.939 when the selection criteria were not applied and between 0.836 and 0.994 when selection was carried out. In biaxial tensile testing, which is more similar to real function, the stress to which the biomaterial is subjected is not likely to align or direct the collagen fibers in a single direction. However, tissue selection enhances the homogeneity of the results, making them predictable [22].

We estimated the curve representing the relationship between the area under the stress/strain curve and the stress applied or the strain produced, respectively, the results of which appear in Table VI and in Figs 3 and 4. They show the energy consumption in relation to the stress applied or the strain produced. As occurred with calf pericardium, this energy is consumed in the production of internal shear stress [23] and in the microdestruction of collagen fibers [11]. We might also hypothesize that there is a limit to the amount of energy that can be spent in each stress/strain cycle without incurring mechanical damage, and that beyond that limit, the internal shear stress can not be absorbed, leading to microfractures in the collagen fibers. These tiny fractures would ultimately be responsible for the rupture and the limited durability of the biomaterial. This is what must take place in the valve leaflets of cardiac bioprostheses, particularly those implanted in mitral position [28], when they have been subjected to intolerable stresses and flow rates over a period of time.

The combination of advances in design engineering and the use of new, more resistant and carefully selected biological materials is the path to follow to achieve a safer bioprosthesis.

Acknowledgments

The authors wish to thank Ms M. Messman for her collaboration, without which the publication of this study would not have been possible. This work was financed by

grant no. MAT2000-0292 from the Spanish Ministry of Science and Technology.

References

1. P. D. KENT, H. D. TAZELAAR, W. D. EDWARDS and T. A. ORSZULAK, *Cardiovasc. Pathol.* **7** (1998) 23.
2. R. DE CASTRO, F. ROQUETTE, R. MARINO, M. MARINO, A. DE CASTRO, W. RABELO and R. CORRÈA, *Ann. Thorac. Surg.* **60** (1995) S316.
3. W. VONGPATANASIN, L. D. HILLIS and R. A. LANGE, *N. Engl. J. Med.* **335** (1996) 407.
4. P. BLOOMFIELD, D. J. WHEATHEY, R. J. PRESCOTT and D. C. MILLER, *ibid.* **324** (1991) 573.
5. G. L. GRUNKEMEIER, W. R. E. JAMIESON, D. C. MILLER and A. STARR, *J. Thorac. Cardiovasc. Surg.* **108** (1994) 709.
6. R. J. LEVY, *J. Heart Valve Dis.* **3** (1994) 101.
7. E. A. TALMAN and D. R. BOUGHNER, *Ann. Thorac. Surg.* **60** (1995) S69.
8. A. C. DUNCAN, D. BOUGHNER and I. VESELY, *Biomaterials* **17** (1996) 1849.
9. G. F. O. TYERS, W. R. JAMIESON, I. A. MUNRO, E. GERMANN, L. H. BURR, R. T. MIYAGISHIMA and L. LING, *Ann. Thorac. Surg.* **60** (1995) S464.
10. S. C. CANNEGIETER, F. R. ROSENDAL and E. BRIET, *Circulation* **89** (1994) 635.
11. M. SACKS, C. CHUONG and R. MORE, *ASAIO J.* **40** (1994) M632.
12. E. D. HIESTER and M. S. SACKS *J. Biomed. Mater. Res.* **39** (1998) 207.
13. E. A. TROWBRIDGE, *Crit. Rev. Biocompatibility* **5** (1989) 105.
14. A. C. DUNCAN, D. BOUGHNER and I. VESELY, *J. Thorac Cardiovasc. Surg.* **113** (1997) 302.
15. J. V. GARCÍA SESTAFE, J. M. GARCÍA PÁEZ, A. CARRERA, E. JORGE, R. NAVIDAD, I. CANDELA and J. L. CASTILLO-OLIVARES, *J. Biomed. Mater. Res.* **28** (1994) 755.
16. J. M. GARCÍA PÁEZ, A. CARRERA, J. V. GARCÍA SESTAFE, E. JORGE, I. MILLAN and I. CANDELA, *Biomaterials* **11** (1990) 186.
17. P. L. GOULD, A. CATALOGIN, P. S. DHATT, A. CHATTOPADHYAY and R. CLARK, in ''Computers and Structures'', vol. 3 (Pergamon Press, London, 1973) p. 377.
18. K. KUNZELMAN, R. P. COCHRAN and E. VERRIER, *J. Med. Impl.* **3** (1993) 161.
19. J. M. GARCIAPÁEZ, A. CARRERA, J. V. GARCIA SESTAFE, E. JORGE HERRERO, I. MILLAN, R. NAVIDAD, A. CORDON and J. L. CASTILLO-OLIVARES, *Biomaterials* **15** (1994) 981.
20. J. M. GARCIA PÁEZ, A. CARRERA, J. V. GARCIA SESTAFE, E. JORGE, I. MILLAN, I. CANDELA and J. L. CASTILLO-OLIVARES, *J. Thorac. Cardiovasc. Surg.* **100** (1990) 580.
21. J. M. GARCIA PÁEZ, A. CARRERA, E. JORGE HERRERO, I. MILLAN, R. NAVIDAD, I. CANDELA, J. V. GARCIA SESTAFE and J. L. CASTILLO-OLIVARES, *Biomaterials* **5** (1994) 172.
22. J. M. GARCÍA PÁEZ, A. CARRERA, E. JORGE, I. MILLAN, A. CORDON, A. ROCHA, J. SALVADOR, J. MENDEZ, N. SANZ and J. L. CASTILLO-OLIVARES, *J. Biomat. Appl.* **15** (2000) 47.
23. E. A. TALMAN and D. R. BOUGHNER, *J. Heart Valve Dis.* **5** (1996) 152.
24. F. GUERRA, U. BORTOLOTTI and G. THIENE, *J. Thorac. Cardiovasc. Surg.* **99** (1990) 838.
25. A. I. MUNRO, W. R. E. JAMIESON, G. F. O. TYERS and E. GERMANN, *Ann. Thorac. Surg.* **59** (1995) S470.
26. D. D. GLOWER, W. D. WHITE, A. C. HATTON, L. R. SMITH, W. G. YOUNG, W. G. WOLFE and J. E. LOWE, *J. Thorac. Cardiovasc. Surg.* **107** (1994) 381.
27. L. H. BURR, R. E. JAMIESSON, A. I. MUNRO, R. T. MIYAGISHIMA and E. GERMANN, *Ann. Thorac. Surg.* **60** (1995) S264.
28. U. BORTOLOTTI, A. MILANO, E. MOSSUTO, E. MAZZARO, G. THIENE and D. CASAROTTO, *J. Heart Valve Dis.* **3** (1994) 81.

Received 20 June
and accepted 1 August 2001